Control of dissipative rogue waves in nonlinear cavity optics: optical injection and time-delayed feedback

Krassimir Panajotov,[1,2] Mustapha Tlidi,[3] Yufeng Song,[4] and Han Zhang[4]

[1)] *Department of Applied Physics and Photonics (IR-TONA), Vrije Universiteit Brussels, Pleinlaan 2, B-1050 Brussels, Belgium*

[2)] *Institute of Solid State Physics, Bulgarian Academy of Sciences, 72 Tzarigradsko Chaussee Blvd., 1784 Sofia, Bulgaria*

[3)] *Faculté des Sciences,Optique Nonlinéaire Thérorique, Université libre de B ruxelles (U.L.B.), C.P. 231, Campus Plaine, B-1050 Bruxelles, Belgium*

[4)] *Shenzhen Engineering Laboratory of Phosphorene and Optoelectronics, Collaborative Innovation Center for Optoelectronic Science and Technology, Institute of Microscale Optoelectronics, Shenzhen University, Shenzhen, 518060 China*

We investigate and we review the formation of two-dimensional dissipative rogue waves in cavity nonlinear optics with transverse effects. Two spatially extended systems are considered for this purpose: the driven Kerr optical cavities subjected to optical injection and the broad-area surface-emitting lasers with a saturable absorber. We also consider a quasi two-dimensional system (the two dimensions being space and time) of fiber laser described the complex cubic-quintic Ginzburg-Landau equation. We show that rogue waves are controllable by mains of time-delay feedback and optical injection. We show that without delay feedback transverse structures are stationary or oscillating. However, when the strength of the delay feedback is increased, all the systems generate giant two-dimensional pulses that appear with low probability and suddenly appear and disappear. We characterize their formation by computing the probability distribution which shows a long tail. Besides, we have computed the significant wave height which measures the mean wave height of the highest third of the waves. We show that for all systems the distribution tails expand beyond two times the significant wave height. Furthermore, we also show that optical injection may suppress the rogue wave formation in a semiconductor laser with saturable absorber.

Rogue waves are observed in many natural systems and they consist of large-amplitude pulses that appear with low probability, unexpectedly and suddenly. In the ocean, rogue waves appear on the surface of the water and may provoke tragic accidents. The long tail probability distribution is the fundamental characteristic of accounting for the generation of rogue waves. The theory of rogue waves either in time or in space has been mainly established in one-dimensional systems in the framework of the nonlinear Schrodinger equation. However, this paradigmatic equation suffers from collapse dynamics and unfortunately, no bounded solution is possible in two or more dimensions. In this contribution devoted to honoring Professor Enrique Tirapegui on the occasion of his 80th anniversary, we investigate the formation of two-dimensional rogue waves in cavity nonlinear optics. Two dissipative systems are considered: the driven Kerr optical cavities subjected to optical injection and the broad-area surface-emitting lasers with saturable absorber. We investigate the control of rogue waves in these systems by the optical injection and time-delayed feedback. We also show that that rogue waves are controllable by mains of time-delay feedback in a quasi two-dimensional system (the two dimensions being space and time) of fiber laser described the complex cubic-quintic Ginzburg-Landau equation.

I. INTRODUCTION

Spatial and/or temporal nonlinear optical cavities support dissipative structures with the explosive growth of the dissipative soliton or localized structures theme, as witnessed by recent overviews[1–13]. In the temporal regime, frequency comb generation in microresonators has witnessed a sudden acceleration in recent years thanks to applications in metrology and spectroscopy[14,15]. Frequency comb generated in Kerr cavity is nothing but the spectral content of stable localized structure occurring in the cavity on the top of low background.

This paper is intended to report on recent progress in control of rogue waves in nonlinear optics. Indeed, during last decade, the studies of rogue waves (RWs) in optics has experienced exponential growth after their first demonstration in fiber optics in 2007[16]. Recent reviews on optical RWs may be found in[17–24,29]. RWs are statistically rare pulses of giant amplitude, much greater with respect to the averaged amplitude of the surrounding waves. They are often called extreme or abnormal events and are characterized by a long tail probability distribution[16,19–21]. RWs in fiber optics are easy to generate in a controlled way experimentally and are well described by the Nonlinear Schrodinger Equation (NLSE)[30] as are also the deep ocean waves[31]. Therefore, they have provided many insight in the origin and properties of ocean RWs - the primary field of RWs interest[31]. The interplay of dispersion and nonlinearity in the NLSE gives rise to modulational instability, i.e. an exponential growth of small perturbations. Modulational instability is an important mechanism for creation of ocean and optical RWs as shown by Peregrine[32]. Indeed, Peregrine solitons have been found experimentally in water wave tank[33,34] and in optical fiber[35,36]. Complicated wave dynamics may also appear as a result of nonlinear interaction between unstable frequencies. For example, interaction between two solutions of the NLSE in the form of Akhmediev breathers and their collision has been studied analytically in[37]. However, NLSE does not admit two-dimensional

solutions due to collapse dynamics. The overwhelming part of optical RW research is in nonilinear fiber optics with recent numerous studies on RWs in fiber lasers[20,21,29,38]. As a matter of fact, RWs are quite universal phenomenon and occur in many fields of optics[21]. Recent studies have shown that spatially extended systems may also exhibit RWs[40–47]. Fiber lasers are an example of dissipative systems that cannot be described by the NLSE. Often, mode locking and RW dynamics in fiber lasers is achieved by inserting a saturable absorber (SA) in the cavity or utilizing nonlinear polarization evolution followed by intensity discrimination in a polarization splitter[27–29,38,39]. Semiconductor lasers with SA also display complex temporal dynamics[48–57]. Alternatively, mode-locking may be achieved by crossed-polarization gain modulation caused by the reinjection of a polarization-rotated replica of the laser output after a time delay[58,59]. Recently, an analysis of rogue waves supported by experimental data in a semiconductor microcavity laser with intracavity saturable absorber has been reported[52,56].

The purpose of this paper is to present the recent progress on theoretical studies of RWs in two-dimensional nonlinear dissipative systems: driven optical cavities subjected to optical injection and broad-area surface-emitting lasers with saturable absorber. In section II we characterize the formation of 2D rogue waves in broad-area surface-emitting laser with a saturable absorber and their control by optical injection and time-delayed feedback. In section III we discuss the occurrence of 2D RWs in the Lugiato-Lefever Model with a delay feedback. In section IV we consider a quasi two-dimensional system (the two dimensions being space and time) of fiber laser described the complex cubic-quintic Ginzburg-Landau equation and show that rogue waves in this system are controllable by mains of time-delay feedback. We conclude in section V.

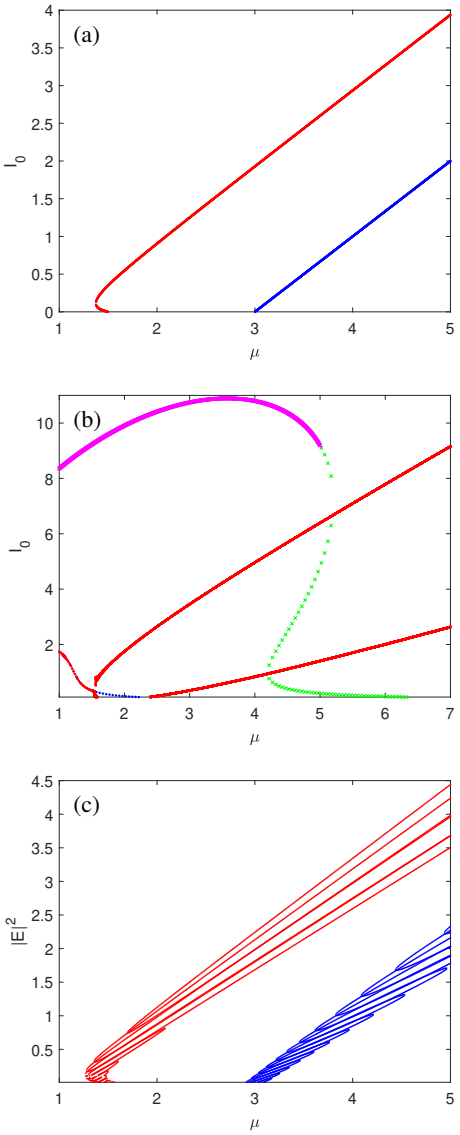

FIG. 1. (colors online) Homogeneous steady state solutions: (a) solitary laser with saturable absorber (Eqn. (7) with parameters A (red) and B (blue); (b) laser with optical injection with $\Delta\omega = 0$ and parameters (A) with $E_i = 1.3$ (blue) and (B) with $E_i = 3.2$ (green) calculated by Eqn. (15). Also shown are bifurcation diagrams (plot of maxima and minima of intensity time-trace) obtained by integration of Eqn. (2)-(3) without the Laplacian: in red - parameter set A and in magenta -parameter set B. (c) Laser with optical feedback with $\eta = 0.1$, $\tau = 50$, $\phi = 0$ and parameters (A) red color; parameters (B) blue color.

II. SURFACE-EMITTING LASER WITH A SATURABLE ABSORBER

It has been numerically demonstrated that a broad-area surface-emitting laser with a saturable absorber is capable of generating two-dimensional spatial rogue waves either by strong pumping[54] or by optical feedback[57]. Experimentally, spatiotemporal chaos and extreme events have been demonstrated in an extended microcavity laser in 1D configuration[52]. Here, we demonstrate that optical injection and time-delayed optical feedback can strongly impact the spatiotemporal dynamics and either suppress or help RW formation. We consider the mean field model describing the space-time evolution of light generated by a broad-area vertical-cavity surface-emitting laser (VCSEL) with saturable absorption[49]. We supplement this model by adding a term $f(E_{inj}, \Delta\omega, \eta, \tau, \phi, E)$ to the equation for the slowly varying electrical field that describes either optical injection or optical feedback

$$\frac{dE}{dt} = \left[(1-i\alpha)N + (1-i\beta)n - 1 + (i+\delta)\nabla_\perp^2\right]E + f(E_{inj}, \Delta\omega, \eta, \tau, \phi, E), \quad (1)$$

$$\frac{dN}{dt} = b_1\left[\mu - N\left(1+|E|^2\right)\right], \quad (2)$$

$$\frac{dn}{dt} = -b_2\left[\gamma + n\left(1+s|E|^2\right)\right]. \quad (3)$$

Here E is the slowly varying mean electric field envelope. N (n) is normalized carrier density, α (β) is the linewidth enhancement factor and b_1 (b_2) is the ratio of photon lifetime to the carrier lifetime in the active layer (saturable absorber) (normalization is the same as in[49]). μ is the normalized injection current in the active material, γ measures absorption in the passive material and $s = a_2 b_1/(a_1 b_2)$ is the saturation parameter with $a_{1(2)}$ the differential gain of the active (absorptive) material. The diffraction of intracavity light E is described by the Laplace operator $\nabla_\perp^2$ acting on the transverse plane (x,y) and complex coefficient in which δ accounts for a phenomenologically introduced diffusion of the electric field that accounts for the final gain bandwidth[48,60]. Carrier diffusion and bimolecular recombination are neglected. Time and space are scaled to the photon lifetime τ_p and diffraction length, respectively.

A. Spatiotemporal dynamics and rogue waves in a solitary laser

Without optical injection or feedback, $f(E_{inj}, \Delta\omega, \eta, \tau, \phi, E) = 0$, the systems of this type have a trivial off solution[49,53]

$$E = 0\,, \qquad N = \mu\,, \qquad n = \gamma, \tag{4}$$

that becomes unstable in a pitchfork bifurcation at the lasing threshold $\mu_{\rm th} = 1+\gamma$. The nontrivial spatially homogeneous steady state solution (HSS) is obtained by using $E = Ae^{i\omega_0 t}$, $I_0 = A^2$ and equating the time derivatives to zero

$$N = \frac{\mu}{1+I_0}\,, \qquad n = -\frac{\gamma}{1+sI_0}, \tag{5}$$

$$i\omega_0 = \frac{\mu(1-i\alpha)}{1+I_0} - \frac{\gamma(1-i\beta)}{1+sI_0} - 1. \tag{6}$$

From the real and imaginary parts of the Eqn. (6) we obtain

$$\frac{\mu}{1+I_0} - \frac{\gamma}{1+sI_0} = 1, \tag{7}$$

$$\omega_0 = \frac{\mu\alpha}{1+I_0} - \frac{\gamma\beta}{1+sI_0} \quad \text{or} \quad \omega_0 = \alpha + \frac{\gamma(\alpha-\beta)}{1+sI_0}. \tag{8}$$

Here ω_0, the lasing frequency for the solitary laser, depends on the intensity I_0 if the linewidth enhancement factors for the active and saturable absorber regions are different. At threshold $\omega_{0,th} = \alpha + \gamma(\alpha-\beta)$.

Due to the saturable absorption the pitchfork bifurcation is subcritical for $s > 1$ with the branch folding in a saddle-node bifurcation at $\mu_{\rm fold} = \left(\sqrt{s-1} + \sqrt{\gamma}\right)^2/s$. This gives rise to a typical S-shape light vs current characteristics, where lasing solutions coexist with a stable off solution - see the red-color curve in Fig. 1(a).

We consider two sets of laser parameters: set (A) $\alpha = 2$, $\beta = 0$, $b1 = 0.04$, $b2 = 0.02$, $\gamma = 0.5$, $s = 10$[51] and set (B) $\alpha = 2$, $\beta = 1$, $b1 = 0.04$, $b2 = 0.04$, $\gamma = 2$, $s = 1$[54]. Injection current μ is control parameter. We integrate numerically Eqs. (1)-(3) by using the standard split-step method with periodic boundary conditions and setting $\delta = 0.01$. It has been shown in[54] that, for the parameter set (B), a stable cavity soliton solution may coexist in a certain region of injection currents with a stable spatiotemporal chaotic solution, a stable nonlasing solution and unstable homogeneous lasing solution. Typical 2D spatial profiles of the chaotic state with apparent extreme events are displayed in Figs. 2(a) and 2(b) for the sets (A) and (B) and $\mu = 1.6$ and $\mu = 3.2$, respectively. The appearance of RWs is also confirmed by the corresponding maximum intensity probability distributions in Fig. 3(a) and 3(b) (red dots): both distribution tails expand beyond the red-dashed lines denoting two times the respective Significant Wave Height (SWH). The SWH is defined as the mean height of the highest third of waves.

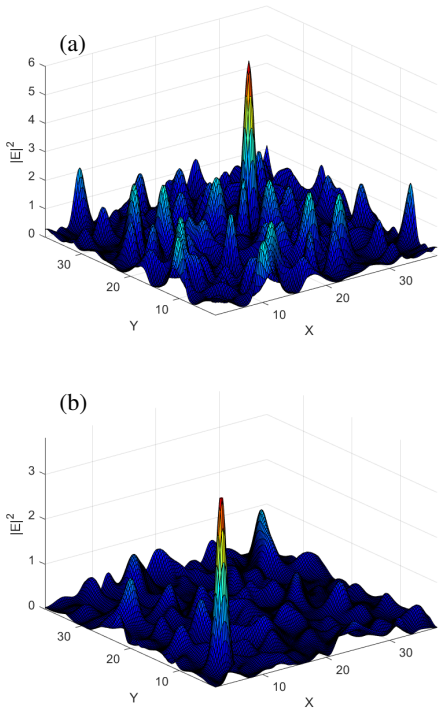

FIG. 2. Snapshots of optical intensity in logarithmic scale for the 2D model of a solitary laser with saturable absorber with an extreme event captured. (a) and (b) correspond to parameter sets (A) and (B) with $\mu = 1.6$ and $\mu = 3.2$, respectively.

B. Optical injection control of spatiotemporal dynamics and rogue waves

The case of optical injection is described by Eqs. (1)-(3) with

$$f(E_{inj}, \Delta\omega, \eta, \tau, \phi, E) = E_{inj} e^{i(\omega_i - \omega_{0,th})t}, \tag{9}$$

where E_{inj} is the strength of the optical injection and $\omega_{inj} - \omega_{0,th} = \Delta\omega$ is the frequency detuning of the injected

monochromatic light with angular frequency ω_{inj} with respect to the solitary laser frequency at threshold $\omega_{0,th} = \alpha + \gamma(\alpha - \beta)$. The explicit time dependence in Eqn. 9 can be removed by subsisting $E = \tilde{E}e^{i(\omega_i - \omega_{0,th})t}$ resulting in

$$\frac{d\tilde{E}}{dt} + i(\omega_i - \omega_{0,th})\tilde{E} = [(1-i\alpha)N + (1-i\beta)n - 1]\tilde{E} + E_{inj}, \tag{10}$$

or

$$\frac{d\tilde{E}}{dt} = [(1-i\alpha)N + (1-i\beta)n - 1 - i\Delta\omega]\tilde{E} + E_{inj}, \tag{11}$$

where $\Delta\omega = \omega_i - \omega_{0,th}$. HSS of the laser when subject to optical injection is found by substituting $\tilde{E} = Ae^{i\Psi}$, equating the time derivative to zero and using Eqn. 5

$$\left[(1-i\alpha)\frac{\mu}{1+A^2} - (1-i\beta)\frac{\gamma}{1+sA^2} - 1 - i\Delta\omega\right] \times A(\cos\Psi + i\sin\Psi) + E_{inj} = 0. \tag{12}$$

Denoting $S_R(A) = \left(\frac{\mu}{1+A^2} - \frac{\gamma}{1+sA^2} - 1\right)A$ and $S_I(A) = \left(-\frac{\alpha\mu}{1+A^2} + \frac{\beta\gamma}{1+sA^2} - \Delta\omega\right)A$ we obtain a system of two nonlinear algebraic equations for the two variables A and Ψ

$$S_R\cos\Psi - S_I\sin\Psi + E_{inj} = 0, \tag{13}$$

$$S_R\sin\Psi + S_I\cos\Psi = 0. \tag{14}$$

Expressing $\tan\Psi = -S_I/S_R$ from Eqn. 14 and replacing it in Eqn. 13 leads to a nonlinear algebraic equation of a single variable A

$$S_R + \frac{S_I^2}{S_R} \pm E_{inj}\sqrt{1 + \frac{S_I^2}{S_R^2}} = 0. \tag{15}$$

Due to the optical injection the previously stable off-branch disappears - see Fig. 1(b). The typical S-shape of the light vs current characteristics for the parameter set (A) - the red-color curves in Fig. 1(a) - also disappears while a Hopf bifurcation leading to time-periodic dynamics becomes evident from the bifurcation diagram (plot of maxima and minima of intensity time-traces) obtained by integration of Eqn. (2)-(3) without the Laplacian - see Fig. 1(b). On the contrary, a reversed hysteresis (switching from high to low intensity with injection current) appears for the parameter set (B) - see the magenta/green-color curves in Fig. 1(b).

Optical injection may also considerably alter the spatiotemporal chaos behavior. In Fig. 3, we demonstrate that optical injection can eliminate the RWs for specific injection parameters. As shown by the blue dotted curves, the pulse maximum amplitude distributions shrink and withdraw in front of the respective 2SHW (dashed blue) lines. Optical injection has been shown to lead to RW generation in small-area (emitting on the fundamental transverse mode) vertical-cavity surface-emitting laser[61]. This happens after the injection locking region is exited for increased injection strength through a region of periodic oscillations, which undergo period doubling

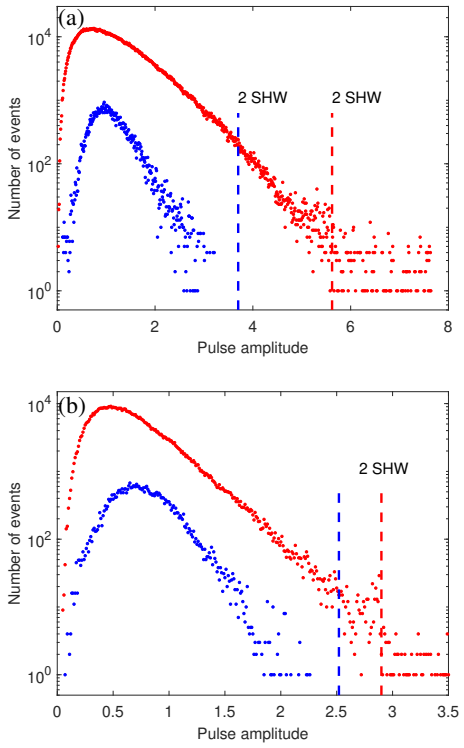

FIG. 3. (color on line) Statistical distributions of pulse height of spatiotemporal chaos in the model of a broad-area surface-emitting laser with a saturable absorber and parameter set: (a) set (A) with $\mu = 1.6$, $E_{inj} = 0$ (red) and $E_{inj} = 1.3$, $\Delta\omega = 0$ (blue); and (b) set (B) with $\mu = 3.2$ and $E_{inj} = 0$ (red) and $E_{inj} = 1.2$, $\Delta\omega = 0$ (blue). The dashed 2SWH lines (twice the significant wave height) denote the corresponding criteria for RWs appearance.

sequence towards chaos. Events with extreme amplitude are observed close to the border but inside the chaotic region.

The impact of the frequency detuning $\Delta\omega$ of the injected light with respect to the solitary laser frequency at threshold is illustrated in Fig. 4 for the two sets A and B of parameters. For the parameter set (A), $\mu = 1.6$ and $E_{inj} = 1.3$ chosen so that the RWs formation is suppressed, introducing a small detuning of $\Delta\omega = 1$ (blue curve) or $\Delta\omega = 2.5$ (green curve) leads to a restoration of the RWs. However, for the parameter set (B) with $\mu = 3.2$ and $E_{inj} = 1.2$, depending on the detuning the system can either stay in a regime of RW formation (the green curve for $\Delta\omega = -10$) or can exit this regime (the blue curve for $\Delta\omega = -5$). In all case, introducing frequency detuning between the injected light and the broad-area laser impacts strongly the observed spatiotemporal dynamics and can efficiently control the RWs formation. For stronger injection and/or larger frequency detuning the spatiotemporal chaos disappears and the laser switches to a homogeneous state stabilized by the optical injection.

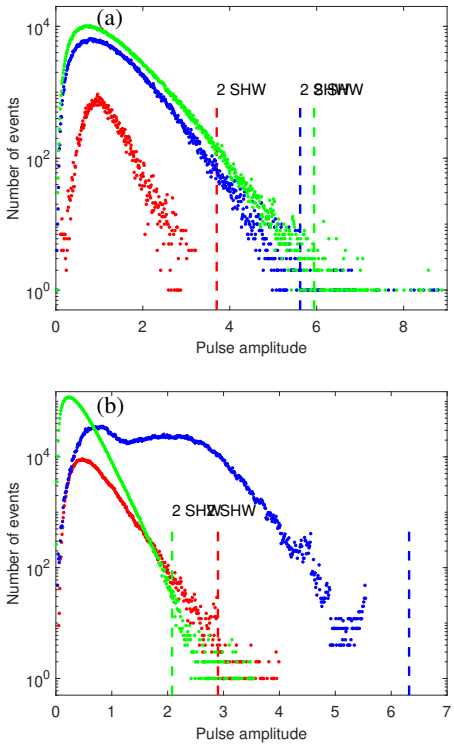

FIG. 4. (color on line) Statistical distributions of pulse height of spatiotemporal chaos in the model of a broad-area surface-emitting laser with a saturable absorber and optical injection illustrating the role of the frequency detuning: (a) set (A) with $\mu = 1.6$ and $E_{inj} = 0$, $\Delta\omega = 0$ (red); $E_{inj} = 1.3$, $\Delta\omega = 1$ (blue); and $E_{inj} = 1.3$, $\Delta\omega = 2.5$ (green).(b) set (B) with $\mu = 3.2$ and $E_{inj} = 0$, $\Delta\omega = 0$ (red); $E_{inj} = 1.2$, $\Delta\omega = -5$ (blue) and $E_{inj} = 1.2$, $\Delta\omega = -10$ (green).

C. Optical feedback control of spatiotemporal dynamics and rogue waves

The case of optical feedback is given by[53,62,63]

$$f(E_{inj}, \Delta\omega, \eta, \tau\phi) = \eta e^{i\phi} E(t-\tau). \tag{16}$$

The optical feedback is described by its strength η, phase ϕ and time delay τ. It is provided by a distant mirror in a self-imaging configuration, i.e. light diffraction in the external cavity is compensated[51]. The time delayed feedback can shift both the threshold pitchfork and the folding bifurcation points. It may also lead to a drift bifurcation so that solitons begin to move[53,64,65,67–69] and to RW formation as recently demonstrated for one-dimensional[21,70,71] and two-dimensional systems[57]. Optical feedback may also induce RWs in small area (single mode) semiconductor lasers in the short-cavity regime, such that the external cavity round-trip time is shorter than the laser relaxation oscillation period[72].

HSSs for the carrier densities in the active medium and saturable absorber sections are the same as Eqns. 5. For the electric field we substitute in Eqn. 2 with the feedback term as given by Eqn. 16, $E \to Ae^{i\Delta\omega t}$ with $\Delta\omega = \omega - \omega_{0,th}$ and $dA/dt = 0$ resulting in

$$i\Delta\omega = (1-i\alpha)N + (1-i\beta)n - 1 + \eta e^{i\phi} e^{-i\Delta\omega\tau}. \tag{17}$$

Separating the real and imaginary parts, we obtain two real equations for two variables I_0 and $\Delta\omega$

$$\frac{\mu}{1+I_0} - \frac{\gamma}{1+sI_0} - 1 + \eta\cos(\Delta\omega\tau - \phi) = 0, \tag{18}$$

$$-\Delta\omega - \alpha\frac{\mu}{1+I_0} + \beta\frac{\gamma}{1+sI_0} - \eta\sin(\Delta\omega\tau - \phi) = 0. \tag{19}$$

These equations are quadratic with respect to I_0. From the first one we obtain

$$\mu(1+sI_0) - \gamma(1+I_0) = (1+sI_0)(1+I_0)\zeta, \quad \text{or} \tag{20}$$
$$\zeta s I_0^2 + (\zeta + \zeta s + \gamma - s\mu)I_0 + \zeta + \gamma - \mu = 0$$

with $\zeta = 1 - \eta\cos(\Delta\omega\tau - \phi)$. Its solutions are

$$I_0 = -b \pm \sqrt{D}, \quad b = (\zeta + \zeta s + \gamma - s\mu)/(2\zeta s), \tag{21}$$
$$D = b^2 - (\zeta + \gamma - \mu)/(\zeta s).$$

These analytical solutions when plugged in Eqn. 19 lead to nonlinear transcendental equations for a single variable $\Delta\omega$. Due to the external cavity multiple solutions of Eqns. 18 and 19 appear, called external cavity modes, which number increases with the delay time τ and feedback strength η[62,63]. Examples of the HSSs for the parameter sets (A) and (B) are shown in Fig. 1(c) for time delay of $\tau = 50$ and $\eta = 0.1$. The single curves from Fig. 1(a) are now split in multiple intertwined curves corresponding to the different external cavity modes.

We consider optical feedback with a time-delay of $\tau = 50$, phase $\phi = 0$ and three feedback strengths: $\eta = 0.1$, $\eta = 0.3$ and $\eta = 0.5$ shown in, respectively, red, blue and green color in Fig. 5. The currents of $\mu = 1.6$ and $\mu = 3.2$ for the (A) and (B) set of parameters are chosen such that the laser operates in the RWs generation regime. In this case, the optical feedback leads to a strong increase of the amplitude of the pulses - see the blue and green curves in Fig 5. Furthermore, the probability of events with amplitude beyond two times the SWH also increases: it changes as 5.5×10^{-5}, 4.9×10^{-5} and 5.3×10^{-5} for the red, blue and green curves, respectively for the parameter set (A) and as 3.7×10^{-5}, 1.33×10^{-4} and 1.31×10^{-4} for the parameter set (B). Alternatively, when the solitary laser is operating in a regime devoid of RWs, the optical feedback may lead to appearance of RWs. In Fig. 6(a) the laser without optical feedback exhibits a subcritical Turing type of bifurcation allowing for the formation of cavity soliton. When the laser is subject to time-delayed feedback the cavity soliton experiences a period-doubling bifurcation to spatially localized chaos[51]. For stronger feedback it enters a regime of spatiotemporal chaos with RWs present - see Fig. 6(b). Statistical analysis of pulse height distribution of spatial-temporal chaos is presented in Fig. 6(c). The long-tailed statistical contribution serves as a signature of the presence of rogue waves: rogue waves with pulse heights more than twice the SWH appear in the system.

III. LUGIATO-LEFEVER MODEL

Another problem which produces stable localized structures in one and in two-dimensional setting[73,74] is a ring cav-

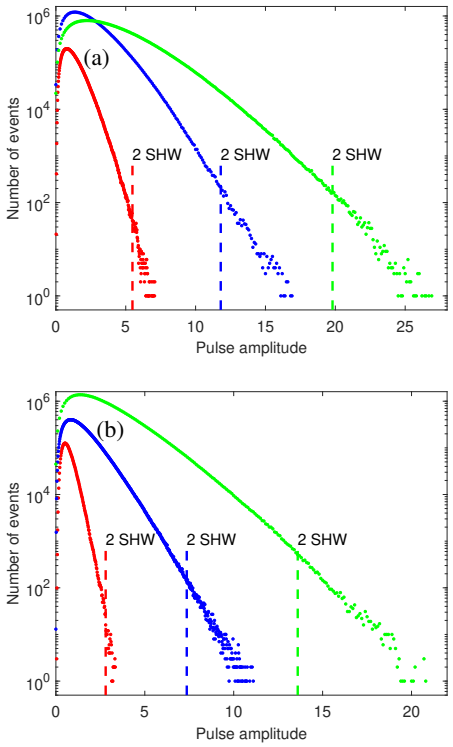

FIG. 5. (color on line) Statistical distributions of pulse height of spatiotemporal chaos in the model of a broad-area surface-emitting laser with a saturable absorber and optical feedback with time delay of $\tau = 50$, phase $\phi = 0$ and three feedback strengths: $\eta = 0.1$ (red); $\eta = 0.3$ (blue) and $\eta = 0.5$ (green). (a) set (A) with $\mu = 1.6$ and (b) set (B) with $\mu = 3.2$.

ity filled with a Kerr media and driven coherently by an external injected signal. This simple device is described by the paradigmatic Lugiato-Lefever equation (LLE,[75]), and it is one the most studied equation in nonlinear optics and in laser physics. Due to the richness of its spectrum of dynamical behaviors, this simple model has attracted considerable theoretical studies. Periodic pattern such as hexagons[76,77], aperiodic localized patterns[73,74,78], fronts propagation[79,80], Eckhaus instability affecting the pattern wavelength[81], and spatiotemporal chaos[82–84] are among the phenomena that have been predicted. In terms of applications, the LLE is the best model for the theoretical investigation of Kerr optical frequency comb generation using integrated ring resonators or whispering gallery mode cavities (see an excellent review on this issue by Lugiato and collaborators[85]).

We propose to investigate the formation of two-dimensional spatial rogue waves based on the time delayed feedback control scheme. To this aim, we implement in the LLE an optical time-delayed feedback[57,64–66] as a single round-trip delay term, i.e. as suggested by Rosanov[86] and Lang and Kobayashi[62]

$$\frac{dE}{dt} = ia\nabla_{\perp}^2 E - (1+i\theta)E + i|E|^2 E + E_i + \eta e^{i\phi} E(t-\tau). \quad (22)$$

Here $E = E(x,y,t)$ is the normalized mean-field cavity electric field, θ is the frequency detuning parameter and losses are

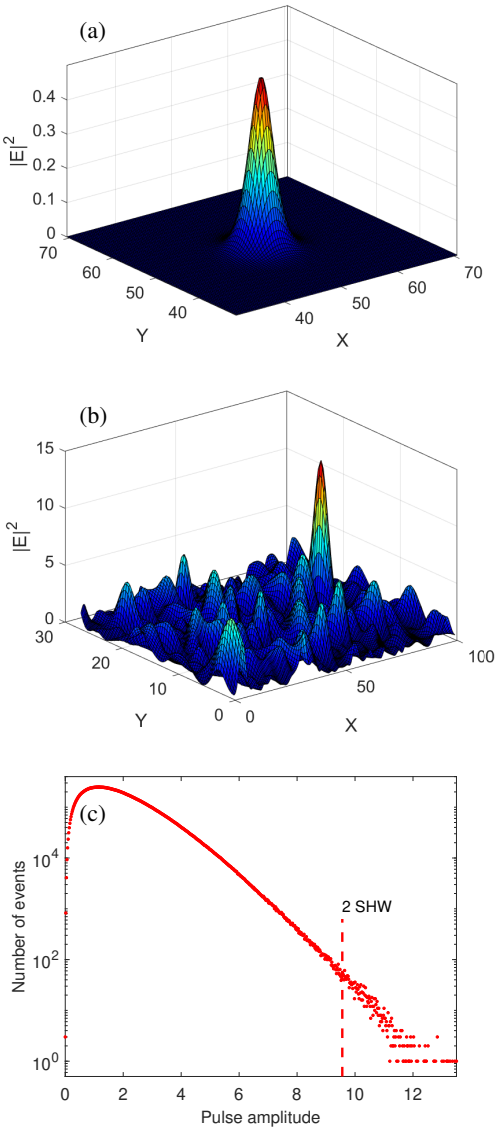

FIG. 6. (color on line) Laser with saturable absorber for injection current of $\mu = 1.45$: snapshots of optical intensity (a) cavity soliton in a solitary laser; (b) laser with optical feedback - an extreme event is captured; (c) statistical distributions of pulse height demonstrating RW generation. Feedback parameters are: time delay $\tau = 50$, phase $\phi = 0$ and feedback strength $\eta = 0.3$.

normalized to unity. Diffraction is modeled by the Laplace operator $\nabla_{\perp}^2$ with diffraction coefficient a. E_i is the input field amplitude assumed to be real and homogeneous, i.e. independent of the transverse coordinates. The delay feedback is modelled by an external cavity operating in a self-imaging configuration[64,65] and is characterized by the time-delay τ, feedback strength η and phase ϕ.

In the absence of delay feedback, the LLE has been derived from other systems such as all-fiber cavities[87] and whispering gallery mode resonators[88]. In these two systems, the diffraction term modeled by the Laplace operator is replaced by a chromatic dispersion effect modeled by a second derivative for the retarded time ξ (slow time) in the reference frame

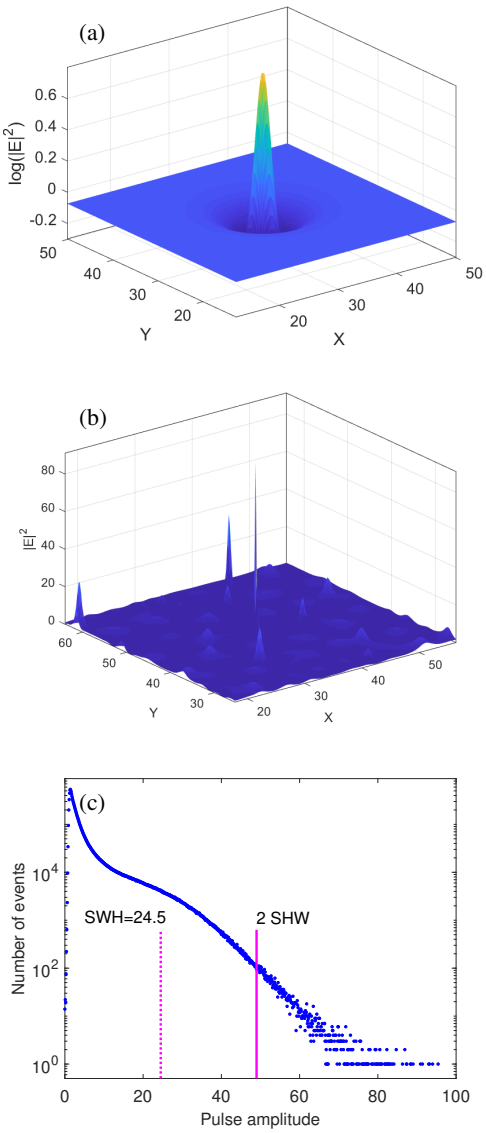

FIG. 7. (color online) (a) Localized structure in the 2D Lugiato-Lefever model without optical feedback. Parameters are $\theta = 1.65$ and $E_i = 1.18$. (b) Spatiotemporal chaos induced by optical feedback: a snapshot of the intensity in the x-y plane with an extreme event captured. (c) Statistical distribution of the pulse height in the spatiotemporal chaos regime with SWH denoting the significant wave height and the dashed line indicating 2 x SWH. Optical feedback parameters are $\eta = 0.2$, $\tau = 10$, and $\phi = 0$.

moving with the group velocity of light. When considering the combined influence of diffraction and chromatic dispersion, the spatiotemporal dynamics of broad area cavities are ruled by the 3D LLE where the Laplace operator acts on the 3D Euclidean space (x, y, ξ)[89–91]. The LLE has also been recovered for a cavity with left-handed materials[92–95] where the diffraction coefficient is negative. More recently, the LLE has been derived from a chain of closely coupled silver nanoparticles embedded in a glass[96].

In the absence of delay feedback, i.e. $\eta = 0$, a single or multipeak stationary localized structures are formed. The existence of stable stationary localized structures does not require a bistable homogeneous response curve. They can be generated in the monostabe regime. The prerequisite condition for their formation is the coexistence between a single homogeneous flat solution and the spatially periodic pattern[73,78]. This coexistence occurs in the monostable regime $41/30 < \theta < \sqrt{3}$. An example of a single stationary localized structure in the monostable regime is shown in Fig. 7(a). The LLE parameters are $\theta = 1.65$, $E_i = 1.18$ and $a = 1 - 0.1i$. The relative stability analysis has shown that the only stable periodic pattern in two-dimensions are hexagons, other symmetries are unstable[77]. The interaction of well-separated bright localized structures has been also discussed[97,98].

The delay feedback may be at the origin of a drift bifurcation leading to motion of a stationary localized structure in variety of optical systems[64,65,67] when the product $\eta\tau$ reaches the value of $+1$ for $\phi = \pi$. This is also the case for the LLE as demonstrated in[68]. It is also shown in[68], that with increasing the strength of the optical feedback the drift bifurcation is followed by an Andronov-Hopf bifurcation, leading to undamped oscillations of the drifting soliton; and latter on by a well-developed spatiotemporal chaotic regime. The appearance of rogue waves in the OF-induced spatiotemporal chaotic dynamics in the LLE is demonstrated in[21].

In high-intensity regime, experiments show evidence of complex spatiotemporal dynamics in whispering gallery mode resonators[99,100] and in all fiber cavities with a Kerr-type media[99,101]. The theoretical characterization of spatiotemporal dynamics have been achieved by computing Lyapunov exponents. From dynamical systems theory, Lyapunov exponents constitute adequate tools that allow not only for the characterization but also for the classification of various complex spatiotemporal behavior such as spatiotemporal chaos, low dimensional chaos, and turbulence. In the former case, the spectrum has a continuous set of positive Lyapunov exponents indicating that the complex behavior observed belongs to the class of spatiotemporal chaos. Two routes to spatiotemporal chaos have been identified either through a period-doubling scenario[82] or through an extended quasiperiodicity[83]. Besides, the Kaplan-Yorke dimension, as an extensive quantity which increases with the system size, has also been estimated[82,83].

Figs. 7(b) and (c) present an example of RWs in a spatiotemporal chaos regime caused by optical feedback in LLE, which, without optical feedback, supports cavity solitons as shown in Fig. 7(a). Optical feedback parameters are $\eta = 0.2$, $\tau = 10$, and $\phi = 0$. Fig. 7(b) shows a snapshot of the intensity in the x-y plane with an extreme event captured. Fig. 7(c) shows a statistical distribution of the pulse height. This figure shows a non Gaussian statistics of the wave intensity, with a long tail of the probability distribution typical for rogue waves formation. Extreme events with amplitude beyond twice the SWH are apparent. This is a remarkable spatiotemporal property found in spatially extended dynamical systems.

Alternatively, RWs can be generated by strong optical injection in LLE without optical feedback[85]. This is demonstrated in Fig. 8(a-b) for $E_i = 2$. Fig. 8(a) shows a snapshot of the intensity in the x-y plane with an extreme event

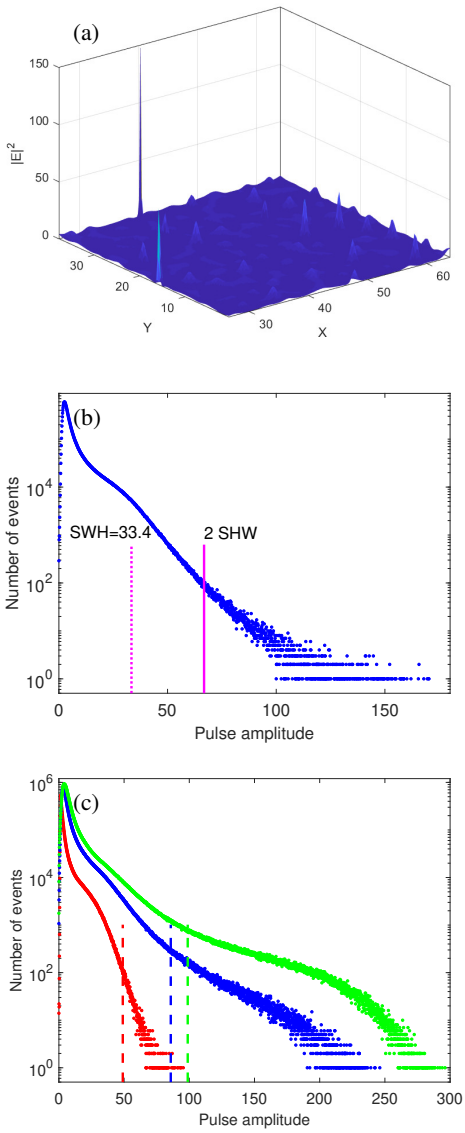

FIG. 8. (color online) RWs generation in spatiotemporal chaos regimes induced by strong optical injection with $E_i = 2$: (a) a snapshot of the intensity in the x-y plane with an extreme event captured and (b) statistical distribution of the pulse height. (c) Comparison of the statistical distribution of the pulse height for the case of optical injection acting alone and optical injection and feedback acting simultaneously: $E_i = 1.18$ $\eta = 0.2$ (red curve); $E_i = 3$ $\eta = 0$ (blue curve); and $E_i = 4$ $\eta = 0.5$ (green curve).

captured and Fig. 8(b) shows a statistical distribution of the pulse height. Fig. 8(c) shows how the statistical distribution of the pulse height in this case is modified if we add optical feedback. It presents a comparison of the statistical distribution of the pulse height for the case of optical injection acting alone and optical injection and feedback acting simultaneously: $E_i = 1.18$ $\eta = 0.2$ (red curve); $E_i = 3$ $\eta = 0$ (blue curve); and $E_i = 4$ $\eta = 0.5$ (green curve). Strong modification of the shoulder of the distribution responsible for high amplitude events clearly occurs when optical injection and feedback act simultaneously.

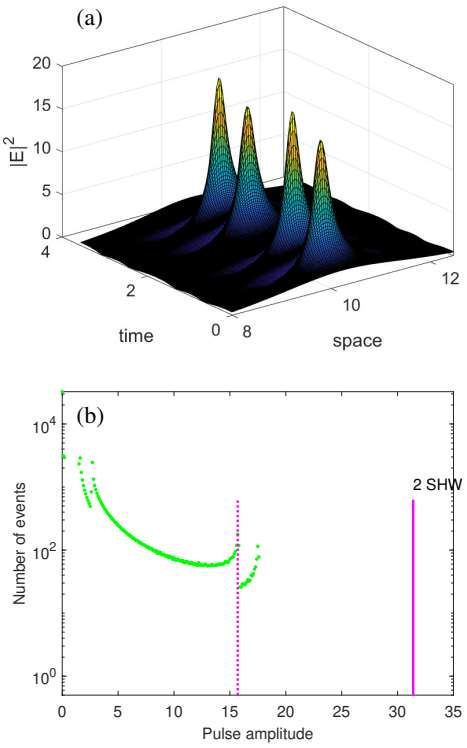

FIG. 9. (color online) Complex cubic-quintic Ginzburg-Landau equation with parameters: $\delta = -0.1$, $D = 1$, $\beta = 0.3$, $\varepsilon = 0.3$, $\mu = -0.001$ and $\nu = 0.1$. (a) a space-time maps of intensity distribution and (b) the corresponding statistical distributions of the pulse height. A laser without optical feedback.

IV. OPTICAL FEEDBACK CONTROL OF EXTREME EVENTS IN FIBER LASER

One of the optical systems in which RWs have been extensively studied both experimentally and theoretically are fiber lasers[29]. Fiber lasers are not only employed in many applications as excellent sources of ultrashort pulses but have led to many discoveries in soliton dynamics; such as, soliton molecules[102], soliton explosion[103], soliton rain[104], rogue waves[39], etc. Often, fiber lasers are modeled by the complex cubic-quintic Ginzburg-Landau equation (CGLE)[103,105–107]. Recently, the CGLE has predicted the existence of dissipative solitons with spikes on top of them that can take extremely large amplitudes[108]. Oscillating and chaotic dissipative soliton have been predicted for the CGLE in[109]. Here, we show that an oscillating soliton dynamics can be substantially impacted by optical feedback converting it to spatiotemporal chaotic dynamics accompanied by rogue wave generation. To this aim, we introduce optical feedback to the CGLE in a similar way as we have done for the case of a nonlinear fiber cavity described by the LLE[71]. The cubic-quintic CGLE with optical feedback reads

$$\frac{\partial E}{\partial z} = \delta E + (\beta + i\frac{D}{2})\frac{\partial^2 E}{\partial t^2} + (\varepsilon + i)|E|^2 E + (\mu + i\nu)|E|^4 E + \eta e^{i\phi} E(t-\tau). \quad (23)$$

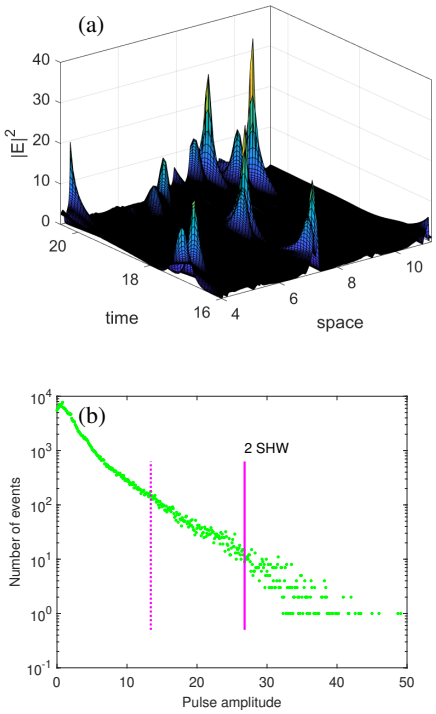

FIG. 10. (color online) Same as Fig. 9 but for a laser with optical feedback with $\eta = 0.5$, $tau = 1$ and $\phi = 0$.

Here, t is the retarded time in the frame moving with the pulse, z is the propagation distance, D is the dispersion, ν is the the saturation coefficient of the Kerr nonlinearity, δ is linear gain-loss difference, ε is the nonlinear gain, β accounts for the spectral filtering and μ is the saturation of the nonlinear gain. Figs. 9 and 10 show the calculations performed by the spilt-step method on Eqn. (24) with parameters: $\delta = -0.1$, $D = 1$, $\beta = 0.3$, $\varepsilon = 0.3$, $\mu = -0.001$ and $\nu = 0.1$. Fig. 9(a) and Fig. 10(a) show snapshots of intensity distribution along the fast time variable t and Fig. 9(b) and Fig. 10(b) show the corresponding statistical distribution of the pulse height. Fig. 9is the case without optical feedback and Fig. 10 is with optical feedback with $\eta = 0.5$, $tau = 1$ and $\phi = 0$. Without feedback the dissipative soliton is oscillating in time as shown in Fig. 9(a). In this case no extreme events are generated as evident by the statistical distribution of the pulse height shown in Fig. 9(b). Applying optical feedback converts the oscillating soliton to spatiotemporal chaos as illustrated in Fig. 10(a). In this case, RWs are generated as evident in Fig. 10(b) by the long-tail of the pulse-height statistical distribution extending beyond the two-time the significant wave height.

RWs in fiber lasers were experimentally studied since 2011[110]. So far, rogue waves with different pulse durations in fiber lasers have been observed[29]. Motivated by soliton study in 2D material-based fiber lasers[111], experimental study on rogue wave also turns to 2D-material based fiber lasers. Moreover, algorithm-controlled fiber lasers are considered as the next generation platform for the study on rogue waves[112]. It is believed that the generating mechanism of rouge waves will be further investigated in pulse fiber lasers with different mode lockers through the intelligent methods in the future.

V. CONCLUSION

We demonstrate generation of two-dimensional optical rogue waves in two generic broad-area nonlinear cavity systems: surface-emitting lasers with a saturable absorber and nonlinear optical resonator subject to optical injection. First, we discussed the modification of the homogeneous steady state solutions by introducing time-delayed optical feedback and optical injection. Next, we have demonstrated that rogue waves can be generated by introducing optical feedback to these systems: while in the absence of delayed feedback the spatial pulses are stationary, for sufficiently strong feedback the systems enter a regime of spatiotemporal chaos leading to formation of rogue waves. Clearly, these rogue waves are exited and controlled by the feedback. For the case of laser with saturable absorber, we have also shown that optical injection may considerably alter the spatiotemporal chaos behavior so that to eliminate the rogue wave generation for specific injection parameters. Finally, we consider a quasi two-dimensional system (the two dimensions being space and time) of fiber laser described the complex cubic-quintic Ginzburg-Landau equation. We demonstrate that time-delay feedback can convert the pulsating soliton dynamics to spatiotemporal chaos with appearing of rogue waves.

ACKNOWLEDGMENTS

This work was supported in part by the Fonds Wetenschappelijk Onderzoek-Vlaanderen FWO (G0E5819N) and the Fonds De La Recherche Scientifique—FNRS in Belgium and the National Natural Science Foundation of China (No. 61705140), and the China Postdoctoral Science Foundation (No. 2018M643165).

[1] F. T. Arecchi, S. Boccaletti, P. Ramazza, Phys. Rep., **318**, 1 (1999).
[2] M. Tlidi, M. Taki, T. Kolokolnikov, Introduction: dissipative localized structures in extended systems, **17**, 037101 (2007).
[3] N. Akhmediev, A. Ankiewicz (Eds.), Dissipative solitons: from optics to biology and medicine, Springer Science & Business Media, 2008.
[4] D. Mihalache, Rom. J. Phys., **57**, 352 (2012).
[5] M. Tlidi, K. Staliunas, K. Panajotov, A. G. Vladimirov, M. G. Clerc, Phil. Trans. Royal Soc. A: Math., Phys. Eng. Sci., **372**, 20140101 (2014).
[6] L. A. Lugiato, F. Prati, and M. Brambilla, Nonlinear optical systems (Cambridge University Press, 2015).
[7] M. Tlidi, M. G. Clerc, Nonlinear dynamics: Materials, theory and experiments, Springer Proceedings in Physics **173** (2016).
[8] D. Mihalache, Rom. Rep. Phys., **69**, 403 (2017).
[9] Y. K. Chembo, D. Gomila, M. Tlidi, C. R. Menyuk, *Theory and applications of the Lugiato-Lefever Equation*, Eur. Phys. J. D **71**, 299 (2017).
[10] M. Tlidi and K. Panajotov, Rom. Rep. Phys **70**, 406 (2018).
[11] M. Tlidi, M. Clerc, K. Panajotov, Dissipative structures in matter out of equilibrium: from chemistry, photonics and biology, the legacy of Ilya Prigogine (part 1), Phil. Trans. Royal Soc. A: Math., Phys. Eng. Sci., **376**, 20180114 (2018).
[12] M. Tlidi, M. Clerc, K. Panajotov, Dissipative structures in matter out of equilibrium: from chemistry, photonics and biology, the legacy of Ilya Prigogine (part 2), Phil. Trans. Royal Soc. A: Math., Phys. Eng. Sci., **376**, 20180276 (2018).

[13]B. Malomed and D. Mihalache, Rom. J. Phys., **64**, 106 (2019).
[14]T. J. Kippenberg, R. Holzwarth, S. A. Diddams, Science, **332**, 555 (2011).
[15]F. Ferdous, H. Miao, D. E. Leaird, K. Srinivasan, J. Wang, L. Chen, L. T. Varghese, A. M. Weiner, Nat. Photon., **5**, 770 (2011).
[16]D.R. Solli, C. Koonath, and B. Jalali, Optical Rogue waves, Nature, **450**, 1054 (2007).
[17]J. M. Soto-Crespo, P. Grelu, N. Akhmediev, Phys. Rev. E, **84**, 016604 (2011).
[18]N. Akhmediev, J. M. Dudley, D.R. Solli, S.K. Turitsyn, J. Opt., **15**, 060201 (2013).
[19]M. Onorato, S. Residori, U. Bortolozzo, A. Montina, F.T. Arecchi, Phys. Rep., **528**, 47 (2013).
[20]M. Dudley, F. Dias, M. Erkintalo, G. Genty, Nature Photonics, **8**, 755 (2014).
[21]N. Akhmediev et al., J. Opt., **18**, 063001 (2016).
[22]A. Ankiewicz and N. Akhmediev, Rom. Rep. Phys **69**, 104 (2017).
[23]S. Chen, F. Baronio, J. Soto-Crespo, P. Grelu, D. Mihalache, J. Phys. A: Math. Theor., **50**, 463001 (2017)
[24]J. M. Dudley, G. Genty, A. Mussot, A. Chabchoub, F. Dias, Nature Rev. Phys., **1**, 675 (2019)
[25]J. M. Soto-Crespo, P. Grelu, N. Akhmediev, Phys. Rev. E, **84**, 016604 (2011).
[26]C. Lecaplain, P. Grelu, J. M. Soto-Crespo, N. Akhmediev, Phys. Rev. Lett., **108**, 233901 (2012).
[27]C. Lecaplain, P. Grelu, J. M. Soto-Crespo, N. Akhmediev, J. Opt., **15**, 064005 (2013).
[28]S. A. Kolpakov, H. Kbashi, S. V. Sergeev, Optica, **3**, 870 (2016).
[29]Y. Song, Z. Wang, C. Wang, K. Panajotov, H. Zhang, "Recent progress on optical rogue wave in fiber lasers: status, challenges and perspectives," submitted to Advanced Photonics.
[30]N. Akhmediev, A. Ankiewicz, M. Taki, Phys. Lett. A, **373**, 675 (2009).
[31]C. Kharif, E. Pelinovsky, A. Slunyaev, Rogue Waves in the Ocean (Springer, 2008).
[32]D.H. Peregrine, J. Australian Math. Soc., Ser. B, **25**, 16 (1983).
[33]A. Chabchoub, N. P. Hoffmann, N. Akhmediev, Phys. Rev. Lett., **106**, 204502 (2011).
[34]A. Chabchoub, N. Akhmediev, N. P. Hoffmann, Phys. Rev. E, **86**, 016311 (2012).
[35]A Mussot, E Louvergneaux, N. Akhmediev, F. Reynaud, L. Delage, M. Taki, Phys. Rev. Lett., **101**, 113904 (2008).
[36]B. Kibler, J. Fatome, C. Finot, G. Millot, F. Dias, G. Genty, N. Akhmediev, J. M. Dudley, Nature Phys., **6**, 790 (2010).
[37]N. Akhmediev, J.M. Soto-Crespo, A. Ankiewicz, Phys. Lett. A, **373**, 2137 (2009).
[38]J. M. Soto-Crespo, P. Grelu, N. Akhmediev, Phys. Rev. E **84**, 016604 (2011).
[39]C. Lecaplain, P. Grelu, J. Soto-Crespo, N. Akhmediev, Phys. Rev. Lett., **108**, 233901 (2012).
[40]V. Odent, M. Taki, E. Louvergneaux, Nat. Hazards Earth Syst. Sci., **10**, 2727 (2010).
[41]F. T. Arecchi, U. Bortolozzo, A. Montina, S. Residori, Phys. Rev. Lett., **106**, 153901 (2011).
[42]S. Birkholz, E.T.J. Nibbering, C. Brée, S. Skupin, A.Demircan, G. Genty, G. Steinmeyer, Phys. Rev. Lett., **111**, 243903 (2013).
[43]A. Montina, U. Bortolozzo, S. Residori, F. T. Arecchi, Phys. Rev. Lett., **103**, 173901 (2009).
[44]P. M. Lushnikov and N. Vladimirova, Opt. Lett., **35**, 1965 (2010).
[45]F. Baronio, M. Conforti, A. Degasperis, S. Lombardo, M. Onorato, S. Wabnitz, Phys. Rev. Lett., **113**, 034101 (2014).
[46]M. Leonetti and C. Conti, Appl. Phys. Lett., **106**, 254103 (2015).
[47]D. Pierangeli, F. Di Mei, C. Conti, A. J. Agranat, E. DelRe, Phys. Rev. Lett., **115**, 093901 (2015).
[48]S. V. Fedorov, A. G. Vladimirov, G. V. Khodova, N. N. Rosanov, Phys. Rev. E, **61**, 5814 (2000).
[49]M. Bache, F. Prati, G. Tissoni, R. Kheradmand, L.A. Lugiato, I. Protsenko, M. Brambilla, Appl. Phys. B, **81**, 913 (2005).
[50]H. Vahed, F. Prati, M. Turconi, S. Barland, G. Tissoni, Phil. Trans. Royal Soc. A, **372**, 2027 (2014).
[51]K. Panajotov and M. Tlidi, Opt. Lett., **39**, 4739 (2014).
[52]F. Selmi, S. Coulibaly, Z. Loghmari, I. Sagnes, G. Beaudoin, M. Clerc, S. Barbay, Phys. Rev. Lett., **116**, 013901 (2016).
[53]C. Schelte, K. Panajotov, M. Tlidi, S. V. Gurevich, Phys. Rev. A, **96**, 023807 (2017).
[54]C. Rimoldi, S. Barland, F. Prati, G. Tissoni, Phys. Rev. A, **95**, 023841 (2017).
[55]K. Panajotov and M. Tlidi, Opt. Lett., **43**, 5663 (2018).
[56]S. Barbay, S. Coulibaly, M. Clerc, Entropy, **20**, 789 (2018).
[57]M Tlidi and K. Panajotov, Chaos, **27**, 013119 (2017).
[58]J. Javaloyes, J. Mulet, S. Balle, Phys. Rev. Lett., **97**, 163902 (2006).
[59]J. Javaloyes, M. Marconi, M. Giudici, Phys. Rev. A, **90**, 023838 (2014).
[60]G.-L. Oppo, A. M. Yao, F. Prati, and G. J. de Valcarcel, Phys. Rev. A, **79**, 033824 (2009).
[61]C. Bonatto, M. Feyereisen, S. Barland, M. Giudici, C. Masoller, J. Leite, J. Tredicce, Phys. Rev. Lett., **107**, 153901 (2011).
[62]R. Lang and K. Kobayashi, IEEE Quantum Electron., **16**, 347 (1980).
[63]K. Panajotov, M. Sciamanna, M. Arizaleta, H. Thienpont, IEEE J. Sel. Top. Quant. Electr., **19**, 1700312 (2013).
[64]M. Tlidi, A. G. Vladimirov, D. Pieroux, D. Turaev, Phys. Rev. Lett., **103**, 103904 (2009).
[65]K. Panajotov and M. Tlidi, European J. Phys. D, **59**, 67 (2010).
[66]M. Tlidi, E. Averlant, A. Vladimirov, K. Panajotov, Phys. Rev. A **86**, 033822 (2012).
[67]A. Pimenov, A. G. Vladimirov, S. V. Gurevich, K. Panajotov, G. Huyet, M. Tlidi, Phys. Rev. A, **88**, 053830 (2013).
[68]K. Panajotov, D. Puzyrev, A. G. Vladimirov, S. V. Gurevich, M. Tlidi, Phys. Rev. A, **93**, 043835 (2016).
[69]B. Kostet, M. Tlidi, F. Tabbert, T. Frohoff-Hülsmann, S. V. Gurevich, E. Averlant, R. Rojas, G. Sonnino, K. Panajotov, Phil. Trans. R. Soc. A, **376**, 20170385 (2018).
[70]M. Tlidi, Y. Gandica, G. Sonnino, E. Averlant, K. Panajotov, Entropy, **18**, 64 (2016).
[71]M Tlidi, K. Panajotov, M. Ferré, M. G. Clerc, Chaos, **27**, 114312 (2017).
[72]J. A. Reinoso, J. Zamora-Munt, C. Masoller, Phys. Rev. E, **87**, 062913 (2013)
[73]A. J. Scorggie, W. J. Firth, G. S. McDonald, M. Tlidi, R. Lefever, L. A. Lugiato, Chaos, Solitons & Fractals, **4**, 1323 (1994).
[74]V. Odent, M. Taki, E. Louvergneaux. New J. Phys., **13**, 113026 (2011).
[75]L. A. Lugiato and R. Lefever, Phys. Rev. Lett., **58**, 2209 (1987).
[76]W. J. Firth, A. J. Scroggie, G. S. McDonald, L.A. Lugiato, Phys. Rev. A, **46**, R3609 (1992).
[77]M. Tlidi, R. Lefever, P. Mandel, Quant. Semiclas. Opt.: J. European Opt. Soc. B, **8**, 931 (1996).
[78]M. Tlidi, P. Mandel, and R. Lefever, Phys. Rev. Lett., **73**, 640 (1994).
[79]S. Coen, M. Tlidi, Ph. Emplit, M. Haelterman, Phys. Rev. Lett. **83**, 2328 (1999).
[80]V. Odent, M. Tlidi, M. G. Clerc, P. Glorieux, E. Louvergneaux, Phys. Rev. A, **90**, 011806(R) (2014).
[81]N. Périnet, N. Verschueren, S. Coulibaly, Europ. Phys. J. D, **71**, 243 (2017).
[82]Z. Liu, M. Ouali, S. Coulibaly, M. Clerc, M. Taki, M. Tlidi, Opt. Lett., **42**, 1063 (2017).
[83]K. Panajotov, M. G. Clerc, M. Tlidi, Europ. Phys. J. D, **71**, 176 (2017).
[84]M. A. Ferré, M. G. Clerc, S. Coulibally, R. G. Rojas, M. Tlidi, Europ. Phys. J. D, **71**, 172 (2017).
[85]L.A. Lugiato, F. Prati, M.L. Gorodetsky, T.J.and Kippenberg. Phil. Trans. Royal Soc. A, **376**, 20180113 (2018).
[86]N. N. Rosanov, Sov. J. Quantum Electronics, vol. 4 (10), 1191 (1975).
[87]M. Haelterman, S. Trillo, S. Wabnitz, Optics Communications **91**, 401 (1992).
[88]Y. K. Chembo and C. R. Menyuk, Phys. Rev. A, **87**, 053852 (2013).
[89]M. Tlidi, M. Haelterman, P. Mandel, Quant. Semiclas. Opt.: J. Europ. Opt. Soc. B, **10**, 869 (1998).
[90]M. Tlidi, M. Haelterman, P. Mandel. Europhys. Lett., **42**, 505 (1998).
[91]N. Veretenov and M. Tlidi, Phys. Rev. A, **80**, 023822 (2009).
[92]P. Kockaert, P. Tassin, G. Van der Sande, I. Veretennicoff, M. Tlidi, Phys. Rev. A, **74**, 033822 (2006).
[93]L. Gelens, G. Van der Sande, P. Tassin, M. Tlidi, P. Kockaert, D. Gomila, I. Veretennicoff, J. Danckaert Phys. Rev. A **75**, 063812 (2007).
[94]M. Tlidi, P. Kockaert, and L. Gelens,Phys. Rev. A **84**, 013807 (2011).

[95]M. Tlidi, C. Fernandez-Oto, M. G. Clerc, D. Escaff, P. Kockaert, Phys. Rev. A, **92**, 053838 (2015).
[96]Z. Ziani, G. Leveque, A. Akjouj, S. Coulibaly, A. Taki, Phys. Rev. B **100**, 165423 (2019).
[97]D. Turaev, A. G. Vladimirov, and S. Zelik, Phys. Rev. Lett. **108**, 263906 (2012).
[98]A. G. Vladimirov, S. V. Gurevich, M. Tlidi, Phys. Rev. A **97**, 013816 (2018).
[99]O. Miguel, S. Resitori, F. Baronio, eds. Rogue and shock waves in nonlinear dispersive media. Vol. 926. Switzerland: Springer, 2016.
[100]Y. K. Chembo, I. S. Grudinin, N. Yu, Phys. Rev. A, **92**, 043818 (2015).
[101]M. Anderson, F. Leo, S. Coen, M. Erkintalo, S. G. Murdoch, Optica, **3**, 1071 (2016).
[102]G. Herink, F. Kurtz, B. Jalali, D. R. Solli, C. Ropers, Science, **356**, 50 (2017).
[103]S. T. Cundiff, J. M. Soto-Crespo, N. Akhmediev, Phys. Rev. Lett., **88**, 073903 (2002).
[104]S. Chouli and P. Grelu, Phys. Rev. A, **81**, 063829 (2010).
[105]J. D. Moores, Opt. Commun., **96**, 65 (1993).
[106]A. Komarov, H. Leblond, F. Sanchez, Phys. Rev. E, **72**, 025604 (2005).
[107]J. Peng, S. Boscolo, Z. Zhao, H. Zeng, Sci. Adv. **5**, 1 (2019).
[108]J. M. Soto-Crespo, N. Devine, N. Akhmediev, J. Opt. Soc. Am. B, **34**, 1542 (2017).
[109]N. Akhmediev, J. M. Soto-Crespo, G. Town, Phys. Rev. E., **63**, 056602 (2001).
[110]A. N. Pisarchik, R. Jaimes-Reategui, R. Sevilla-Escoboza, G. Huerta-Cuellar, M. Taki, Phys. Rev. Lett., **107**, 274101 (2011).
[111]Y. F. Song, X. J. Shi, C. F. Wu, D. Y. Tang, H. Zhang, Appl. Phys. Rev. (USA), **6**, 021313 (2019).
[112]G. Pu, L. Yi, L. Zhang, W. Hu, Optica, **6**, 362 (2019).